The effect of Au cocatalyst loaded on La-doped NaTaO$_3$ on photocatalytic water splitting and O$_2$ photoreduction

Akihide Iwase [a,b], Hideki Kato [a,1], Akihiko Kudo [a,b,*]

[a] Department of Applied Chemistry, Faculty of Science, Tokyo University of Science, 1–3 Kagurazaka, Shinjuku-ku, Tokyo, 162-8601, Japan
[b] Division of Photocatalyst for Energy and Environment, Research Institute of Science and Technology, Tokyo University of Science, Tokyo, Japan

ABSTRACT

Photocatalytic water splitting over La-doped NaTaO$_3$ (NaTaO$_3$:La) was improved by loading with Au cocatalyst which works as H$_2$ evolution sites. NaTaO$_3$:La loaded with Au by an impregnation method showed higher and more steady activity for water splitting than that by a photodeposition method. This difference in the activity for water splitting was related to the O$_2$ photoreduction on the loaded Au cocatalyst, which is one of the backward reactions of water splitting. The impregnated spherical Au cocatalyst suppressed the O$_2$ photoreduction by photogenerated electrons more efficiently than the photodeposited hemispherical Au cocatalyst, because the perimeter of Au/NaTaO$_3$:La interface which produces activated O$_2$ molecules was smaller in the impregnated Au than the photodeposited Au.

© 2013 Elsevier B.V. All rights reserved.

1. Introduction

Hydrogen is one of the promising clean energy sources to address the energy and environmental issues. Photocatalytic water splitting has been extensively studied as an effective and clean way to obtain hydrogen. Although many photocatalysts for water splitting have been reported [1–3], most of them require cocatalysts. Some exceptions include A$_4$Nb$_6$O$_{17}$ (A: K and Rb) [4,5] which possesses unique reaction sites at the interlayer and some tantalates as well as ZrO$_2$ that has large driving force for H$_2$ evolution caused by the high conduction band [6–10]. In other words, the reaction sites and driving forces for water reduction and oxidation are very important factors for photocatalytic water splitting.

Essentially, cocatalyst introduces two positive factors into the photocatalyst; (i) promotion on the separation of photogenerated electrons from holes and (ii) construction of active sites for reduction or oxidation reaction. Since both reduction and oxidation reactions take place on the surface of one photocatalyst particle, the cocatalyst contributing to the above factors plays an important role in photocatalysis. Metal oxides, such as NiO [11], RuO$_2$ [12,13] and Rh-Cr oxide [14], have been commonly used as cocatalysts for photocatalytic water splitting. Well-known Pt

[15–17] and Rh [18,19] metal cocatalysts are not suitable for water splitting, because a backward reaction of water splitting, H$_2$ + O$_2$ → H$_2$O, is promoted on these cocatalysts. In such background, we have preliminary reported that Au loaded by photodeposition method functions as a metallic cocatalyst for water splitting [20].

Au has attracted extensive attention as a useful material for biosensor and photofunctional devices. In contrast to the bulky Au, Au fine particle possesses typical properties such as magnetism [21] and surface plasmon absorption [22]. Additionally, the Au fine particle is also useful for thermocatalytic oxidation [23–27]. The activity increases with reducing the size of Au particle [24], and the shape of Au particle affects the selectivity of the oxidation reaction [23,26]. The shape and size of Au particle can be controlled by loading method. It has been also reported that the loading method affects the photocatalytic activity for H$_2$ evolution over Au-loaded photocatalysts in the presence of a hole scavenger [28,29].

In the present study, the effect of the loading method of Au cocatalyst on the highly active NaTaO$_3$:La photocatalyst for water splitting was investigated. The effects of the shape and size of loaded Au particle on water splitting are also discussed.

2. Experimental

NaTaO$_3$ powder doped with 2 mol.% of La was prepared by a solid state reaction according to the previous report [8]. Au cocatalyst was loaded by photodeposition and impregnation methods using an aqueous solution of HAuCl$_4$·4H$_2$O (Wako Pure Chemical; 99%). Photodeposition of Au was carried out using an aqueous solution

---

Table 1
Photocatalytic overall water splitting on Au-loaded $NaTaO_3$:La powder.

Loading method	Amount of loaded Au (wt.%)	Rate of gas evolution ($\mu mol\,h^{-1}$)	
		H_2	O_2
Non-loading	0	404	187
Photodeposition	0.3	498	133
Photodeposition	1	2890	1190
Photodeposition	3	2820	1220
Impregnation	0.3	4120	1920
Impregnation	1	6910	3320
Impregnation	3	7290	3470

Photocatalyst: 0.3–0.5 g, reactant solution: water 350 mL, reaction cell: inner irradiation cell made of quartz, light source: 400-W high-pressure Hg lump.

containing a certain amount of $HAuCl_4$, *in situ*, during the photocatalytic reaction. For impregnation of Au, $NaTaO_3$:La powder and an aqueous $HAuCl_4$ solution was mixed in a porcelain crucible, and the dispersion was heated on a hot plate until all water vaporized. The $NaTaO_3$:La powder impregnated with $HAuCl_4$ was treated with hydrogen (1 atm) at 373–573 K for 1–2 h to obtain metallic Au-loaded $NaTaO_3$:La.

Photocatalytic reactions were carried out in a gas-tight circulation system. For overall water splitting, the photocatalyst powder (0.3–0.5 g) was dispersed in water (350 mL). An inner irradiation cell made of quartz and a 400-W high-pressure Hg lamp (SEN; HL400EH-5) were employed. The half reactions of water splitting, *i.e.*, sacrificial H_2 and O_2 evolution, were also examined from aqueous solutions of methanol and silver nitrate, respectively, using a top-irradiation cell with a quartz window and a 300-W Xe lamp (PerkinElmer, CERMAX LX-300BUV). The amounts of evolved H_2 and O_2 were determined with gas chromatography (TCD, MS-5A, Ar carrier gas) which was directly connected to a gas sampling port attached to the gas-tight circulation system.

A backward reaction between H_2 and O_2 to produce water in a gas phase was investigated. Photocatalyst powder (0.1 g) and a gas mixture of H_2 (100 Torr) and O_2 (50 Torr) were introduced into a gas-tight circulation system with 350-mL of a dead volume. The decreases in the pressure of the gases were monitored by gas chromatography.

Diffuse reflectance spectra were obtained with a UV–vis–NIR spectrometer (JASCO, Ubest-570) and were converted from reflectance to absorbance by the Kubelka–Munk method. The photocatalysts were observed by a scanning electron microscope (JEOL, JSM-6700F) and a transmission electron microscope (JEOL, JEM-2000F).

3. Results and discussion

3.1. Photocatalytic activities over $NaTaO_3$:La loaded with Au-cocatalyst by photodeposition and impregnation methods

Table 1 shows photocatalytic overall water splitting on $NaTaO_3$:La loaded with Au-cocatalyst by photodeposition and impregnation methods. Bare $NaTaO_3$:La photocatalyst showed activity for water splitting. The photocatalytic activity was improved when Au-cocatalyst was loaded by both photodeposition and impregnation methods. Although the activities for water splitting were improved with increasing the amount of loaded Au, they saturated at 1 wt.% of Au to $NaTaO_3$:La. When more than 3 wt.% of Au was attempted to be loaded by the photodeposition method, aggregated Au particles were separated from $NaTaO_3$:La powder, indicating that excessive Au could not be loaded. Impregnated Au(1 wt.%) cocatalyst improved the photocatalytic water splitting activity of $NaTaO_3$:La by 17 times, while photodeposited Au(1 wt.%) cocatalyst improved by 7 times. The difference between
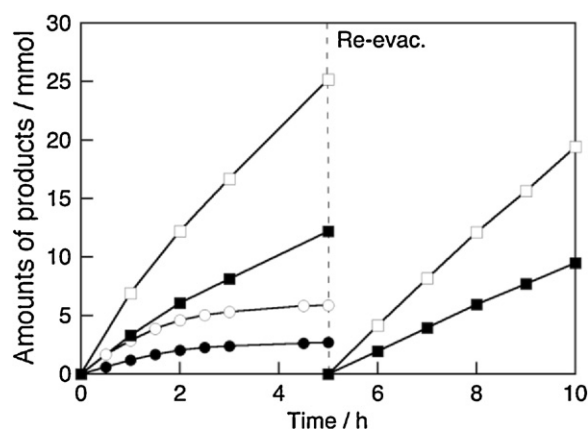

Fig. 1. Photocatalytic water splitting into H_2 and O_2 over Au(1 wt.%)/$NaTaO_3$:La-photo (circle) and Au(1 wt.%)/$NaTaO_3$:La-imp (square). H_2: open marks, O_2: closed marks. Photocatalyst: 0.5 g, pure water: 350 mL, 400-W high-pressure Hg lamp, inner irradiation cell made of quartz.

impregnated and photodeposited Au cocatalysts was observed not only for the enhancement in activity but also on the gas-evolving profiles as shown in Fig. 1. Fig. 1 shows time courses of overall water splitting over $NaTaO_3$:La loaded with Au(1 wt.%) by a photodeposition (Au(1 wt.%)/$NaTaO_3$:La-photo) and an impregnation (Au(1 wt.%)/$NaTaO_3$:La-imp) methods in a gas-tight circulation system in which evolved H_2 and O_2 accumulated. The activity of Au(1 wt.%)/$NaTaO_3$:La-photo decreased gradually with the reaction time, while Au(1 wt.%)/$NaTaO_3$:La-imp showed higher and more stable photocatalytic activity. Thus, it was found that the impregnation method was useful for loading the Au-cocatalyst for water splitting.

Table 2 shows H_2 and O_2 evolution over Au(1 wt.%)/$NaTaO_3$:La-photo and Au(1 wt.%)/$NaTaO_3$:La-imp from aqueous solutions in the presence of methanol and $AgNO_3$ as the sacrificial reagents, respectively. Both impregnated and photodeposited Au promoted H_2 evolution over $NaTaO_3$:La, while no enhancement was observed for O_2 evolution. Additionally, we have reported that Au-loaded $SrTiO_3$ showed photocatalytic activity for H_2 evolution in the presence of methanol, but bare $SrTiO_3$ did not [20]. These results indicate that the Au-cocatalyst works as an active site for H_2 evolution, as previously reported [20,28,29].

3.2. The effect of O_2 on water splitting over $NaTaO_3$:La loaded with Au-cocatalyst by photodeposition and impregnation methods

To clarify the reason for the difference in the behavior of water splitting between Au(1 wt.%)/$NaTaO_3$:La-photo and

Table 2
Photocatalytic H_2 and O_2 evolution from aqueous methanol and $AgNO_3$ solutions over $NaTaO_3$:La loaded with Au(0.3 wt.%) by photodeposition and impregnation methods.

Loading method	Reactant solution	Rate of gas evolution ($\mu mol\,h^{-1}$)	
		H_2	O_2
Non-loading	CH_3OH[a]	191	–
Non-loading	$AgNO_3$[b]	–	44
Photodeposition	CH_3OH[a]	451	–
Photodeposition	$AgNO_3$[b]	–	40
Impregnation	CH_3OH[a]	388	–
Impregnation	$AgNO_3$[b]	–	40

Photocatalyst: 0.3 g, reactant solution: 120 mL, 300-W Xe lamp, top-irradiation cell with a quartz window.

[a] 10 vol.% CH_3OH aq.
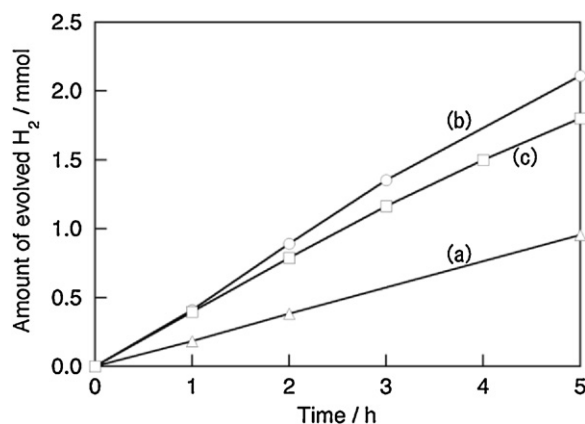
[b] 0.02 mol. L^{-1} $AgNO_3$ aq.

Fig. 2. Photocatalytic H_2 evolution from aqueous methanol solution over (a) non-loaded $NaTaO_3$:La, (b) Au(0.3 wt.%)/$NaTaO_3$:La-photo and (c) Au(0.3 wt.%)/$NaTaO_3$:La-imp. Photocatalyst: 0.3 g, reactant solution: 10 vol.% methanol 120 mL, 300-W Xe lamp, top-irradiation cell with a quartz window.

Au(1 wt.%)/$NaTaO_3$:La-imp as observed in Fig. 1, we have examined the H_2 evolution from an aqueous methanol solution, and the backward reaction between H_2 and O_2 as shown in Figs. 2 and 3. H_2 evolved steadily from an aqueous methanol solution regardless of the loading method (Fig. 2), being different from water splitting over Au(1 wt.%)/$NaTaO_3$:La-photo (Fig. 1). Moreover, the photodeposited Au cocatalyst was more active than the impregnated Au cocatalyst for the sacrificial H_2 evolution accompanied with no O_2 evolution, in contrast to water splitting. These results indicate that the evolved O_2 during water splitting induced the deactivation of water splitting over Au(1 wt.%)/$NaTaO_3$:La-photo. However, no backward reaction between H_2 and O_2 under dark condition proceeded on the photodeposited and impregnated Au cocatalysts as observed in Fig. 3. Therefore, it was suggested that the rate of O_2 reduction by photogenerated electrons over the Au-cocatalyst would be different between Au(1 wt.%)/$NaTaO_3$:La-photo and Au(1 wt.%)/$NaTaO_3$:La-imp, resulting in the difference in water splitting behavior as observed in Fig. 1.

To confirm the effect of O_2 on photocatalytic reactions over Au(1 wt.%)/$NaTaO_3$:La-photo and Au(1 wt.%)/$NaTaO_3$:La-imp, O_2 gas was introduced into a gas-tight circulation system prior to the photocatalytic reactions of overall water splitting and H_2 evolution from an aqueous methanol solution as observed in Fig. 4. As shown in Fig. 4a, the overall water splitting on Au(1 wt.%)/$NaTaO_3$:La-photo was suppressed drastically in the presence of O_2, while
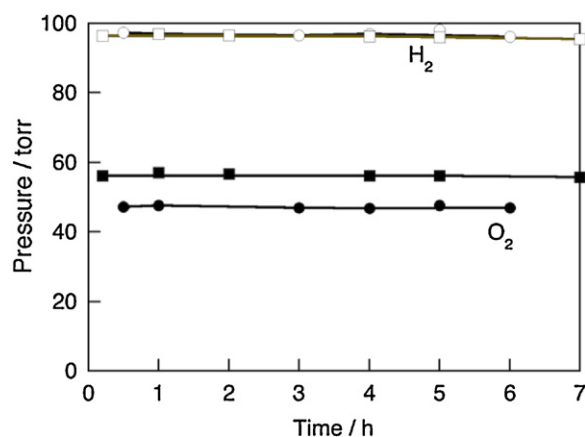

Fig. 3. Backward-reaction between H_2 and O_2 to produce water in a gas phase in dark over Au(1 wt.%)/$NaTaO_3$:La-photo (circle) and Au(1 wt.%)/$NaTaO_3$:La-imp (square). Photocatalyst: 0.1 g.
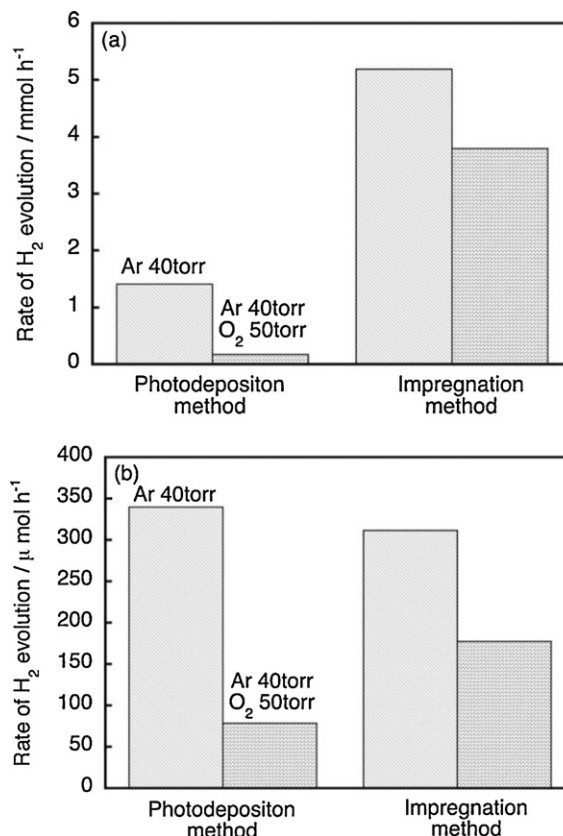

Fig. 4. (a) Effect of O_2 addition on overall water splitting over Au(1 wt.%)/$NaTaO_3$:La-photo, and Au(1 wt.%)/$NaTaO_3$:La-imp. Photocatalyst: 0.5 g, pure water: 350 mL, 400-W high pressure Hg lamp, inner irradiation cell made of quartz. (b) Effect of O_2 addition on H_2 evolution from an aqueous methanol solution over Au(1 wt.%)/$NaTaO_3$:La-photo, and Au(1 wt.%)/$NaTaO_3$:La-imp. Catalyst: 0.3 g, reactant solution: 10 vol.% methanol 120 mL, 300-W Xe lamp, top-irradiation cell with a quartz window.

Au(1 wt.%)/$NaTaO_3$:La-imp still maintained the high activity. A similar result was also observed for H_2 evolution from an aqueous methanol solution as shown in Fig. 4b; the decrease in the activity of Au(1 wt.%)/$NaTaO_3$:La-photo by introducing O_2 was much larger than that of Au(1 wt.%)/$NaTaO_3$:La-imp. Thus, the photocatalytic water splitting and H_2 evolution over Au(1 wt.%)/$NaTaO_3$:La-photo was suppressed by O_2 more efficiently than those over Au(1 wt.%)/$NaTaO_3$:La-imp. In other words, the photocatalytic reduction of O_2 over Au(1 wt.%)/$NaTaO_3$:La-photo proceeded more efficiently than that of Au(1 wt.%)/$NaTaO_3$:La-imp.

3.3. Photoreduction of O_2 over Au surface

Haruta et al. claimed that the periphery of Au particles contacted with supports can activate O_2 molecules [26]. In our case, since Au particle works as H_2 evolution site, the activated O_2 molecule at the periphery may easily react with H atom adsorbed on Au particle surface to form water. Therefore, the rate of photoreduction of O_2 should depend on the total area of perimeter interface between the loaded Au and $NaTaO_3$:La particles.

The particle size and shape of loaded Au affect the total area of the perimeter interface. The Au(1 wt.%)/$NaTaO_3$:La-photo and the Au(1 wt.%)/$NaTaO_3$:La-imp were characterized by TEM, SEM, UV–vis–IR spectroscopy, and XPS to determine the size and shape of the loaded Au. TEM and SEM observation revealed that the photodeposited Au was hemispherical particles, while the impregnated Au was spherical particles as shown in Fig. 5. A hemispherical Au particle photodeposited gave larger perimeter interface than
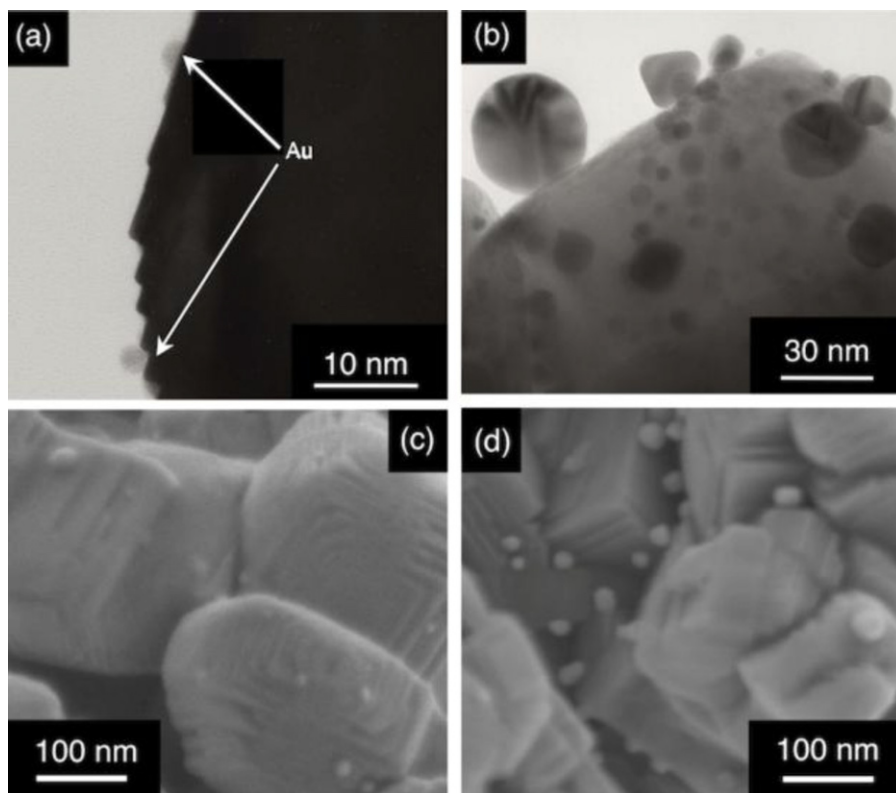
Fig. 5. TEM and SEM images of (a, c) Au(1 wt.%)/NaTaO$_3$:La-photo and (b, d) Au(1 wt.%)/NaTaO$_3$:La-imp.

a spherical Au particle impregnated. Additionally, the average size of the photodeposited Au (5–20 nm) particles was smaller than that of the impregnated Au (5–40 nm) particles, as shown in Fig. 6. This difference in the particle size corresponded well to their surface plasmon absorption bands in the UV–vis spectra as shown in Fig. 7. Au(1 wt.%)/NaTaO$_3$:La-photo showed a sharp surface plasmon absorption band at around 530 nm, while Au(1 wt.%)/NaTaO$_3$:La-imp exhibited a broad surface plasmon absorption band at around 550 nm. The position of absorption band is dependent on the size of Au fine particles, and the shift in the absorption peak from 530 nm to 550 nm was due to the increase in the size of loaded Au particles. Furthermore, the difference in the particle size indicated that the number of photodeposited Au island on the NaTaO$_3$:La was larger than that of impregnated Au island, since the same amount of Au was loaded. XPS measurement also indicated that the ratio of Au at the surface of Au(1 wt.%)/NaTaO$_3$:La-photo (Au/Ta = 0.054) was larger than that of Au(1 wt.%)/NaTaO$_3$:La-imp (Au/Ta = 0.040), meaning that the photodeposited Au cocatalyst was dispersed better than the impregnated Au cocatalyst.

Based on the results of TEM, UV–vis–IR spectroscopy, and XPS, the schematic view of the photodeposited and impregnated Au cocatalysts are depicted in Fig. 8. The total length of the perimeter interface at Au(1 wt.%)/NaTaO$_3$:La-photo with small and hemispherical Au particles was larger than that at Au(1 wt.%)/NaTaO$_3$:La-imp with large spherical Au particles. The larger perimeter interface produces more activated O$_2$ molecules, resulting in an enhancement of the backward reaction involving the oxidization of adsorbed H atoms on the Au surface. Therefore, the water splitting activity of Au(1 wt.%)/NaTaO$_3$:La-photo was gradually reduced with the reaction time, unlike Au(1 wt.%)/NaTaO$_3$:La-imp.

The another considerable reason why the O$_2$ reduction ability is different between Au(1 wt.%)/NaTaO$_3$:La-photo and Au(1 wt.%)/NaTaO$_3$:La-imp is the electronic states of loaded Au
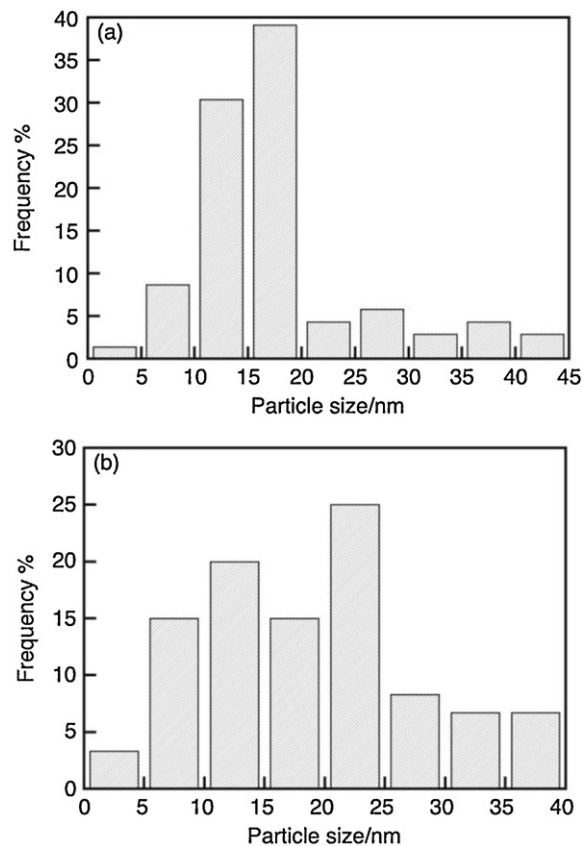

Fig. 6. Size distributions of the gold particles in (a) Au(1 wt.%)/NaTaO$_3$:La-photo and (b) Au(1 wt.%)/NaTaO$_3$:La-imp. Particle size and frequency were estimated by direct observation of TEM and SEM.
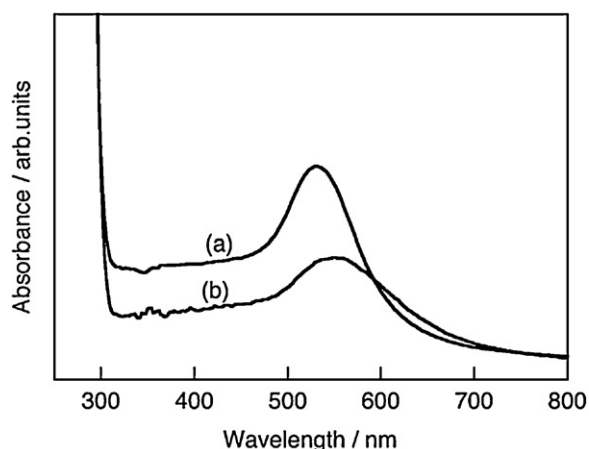
Fig. 7. Diffuse reflectance spectra of (a) Au(1 wt.%)/NaTaO$_3$:La-photo and (b) Au(1 wt.%)/NaTaO$_3$:La-imp.
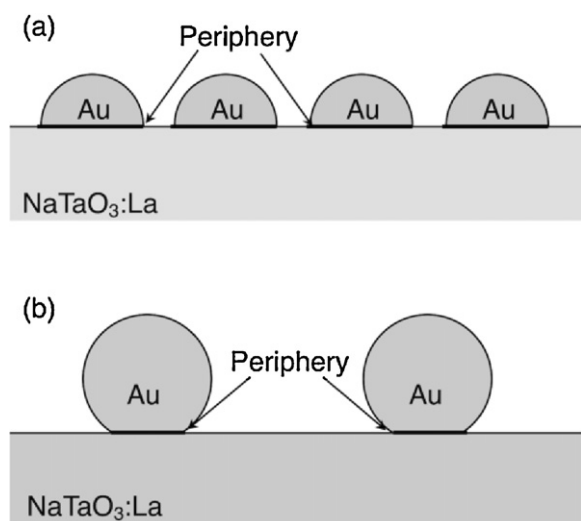

Fig. 8. Schematic views of (a) photodeposited and (b) impregnated Au on NaTaO$_3$:La.

cocatalyst particles. The difference in the electronic states was indicated by the different positions of surface plasmon absorption bands, as shown in Fig. 7.

4. Conclusions

Water splitting activity of NaTaO$_3$:La was improved when Au was loaded by photodeposition and impregnation methods. Based on the half reactions of water splitting which were the H$_2$ and O$_2$ evolution in the presence of sacrificial reagents, the loaded Au cocatalyst worked as H$_2$ evolution sites. Au/NaTaO$_3$:La prepared by an impregnation method showed higher and more stable activity for water splitting, while the water splitting over Au/NaTaO$_3$:La prepared by a photodeposition method decelerated with the reaction time. This difference in the photocatalytic activity was due to the O$_2$ reduction on the loaded Au cocatalyst; O$_2$ reduction on

photodeposited Au cocatalyst was more efficiently than that of impregnated Au cocatalyst. Periphery of the interface between Au and NaTaO$_3$:La works for O$_2$ activation. The photodeposited Au particles with small hemisphere introduced a larger periphery than the impregnated Au particles with large sphere. Moreover, the difference in the electronic states might affect the ability of the O$_2$ activation. Thus, we successfully controlled the size and shape of Au cocatalyst by changing the loading method, leading to different activities for water splitting and O$_2$ reduction.

Appendix A. Supplementary data

Supplementary data associated with this article can be found, in the online version, at http://dx.doi.org/10.1016/j.apcatb.2013.02.006.

References

[1] H.E. Osterloh, Chemistry of Materials 20 (2008) 35–54.
[2] A. Kudo, Y. Miseki, Chemical Society Reviews 38 (2009) 253–278.
[3] Y. Inoue, Energy and Environmental Science 2 (2009) 364–386.
[4] A. Kudo, K. Sayama, A. Tanaka, K. Asakura, K. Domen, K. Maruya, T. Onishi, Journal of Catalysis 120 (1989) 337–352.
[5] K. Sayama, H. Arakawa, K. Domen, Catalysis Today 28 (1996) 175–182.
[6] K. Sayama, H. Arakawa, Journal of Physical Chemistry 97 (1993) 531–533.
[7] M. Machida, J. Yabunaka, T. Kijima, Chemistry of Materials 12 (2000) 812–817.
[8] H. Kato, K. Asakura, A. Kudo, Journal of the American Chemical Society 125 (2003) 3082–3089.
[9] H. Otsuka, K. Kim, A. Kouzu, I. Takimoto, H. Fujimori, Y. Sakata, H. Imamura, T. Matsumoto, K. Toda, Chemistry Letters 34 (2005) 822–823.
[10] A. Iwase, H. Kato, A. Kudo, ChemSusChem 2 (2009) 873–877.
[11] K. Domen, S. Naito, S. Soma, M. Onishi, K. Tamaru, Journal of the Chemical Society, Chemical Communications (1980) 543–544.
[12] T. Kawai, T. Sakata, Chemical Physics Letters 72 (1980) 87–89.
[13] J. Sato, N. Saito, H. Nishiyama, Y. Inoue, Journal of Physical Chemistry B 107 (2003) 7965–7969.
[14] K. Maeda, K. Teramura, D. Lu, T. Takata, N. Saito, Y. Inoue, K. Domen, Nature 440 (2006) 295.
[15] S. Sato, J.M. White, Journal of Catalysis 69 (1981) 128–139.
[16] K. Sayama, H. Arakawa, Journal of Photochemistry and Photobiology A 77 (1994) 243–247.
[17] S. Tabata, N. Nishida, Y. Masaki, K. Tabata, Catalysis Letters 34 (1995) 245–249.
[18] J.P. Lehn, J.P. Sauvage, R. Ziessel, Nouveau Journal de Chimie 4 (1980) 623–627.
[19] K. Yamaguchi, S. Sato, Journal of the Chemical Society, Faraday Transactions 1 (81) (1985) 1237–1246.
[20] A. Iwase, H. Kato, A. Kudo, Catalysis Letters 108 (2006) 7–10.
[21] Y. Yamamoto, T. Miura, M. Suzuki, N. Kawamura, H. Miyagawa, T. Nakamura, K. Kobayashi, T. Teranishi, H. Hori, Physical Review Letters 93 (2004) 116801.
[22] S. Link, M.J. El-Sayed, Journal of Physical Chemistry B 103 (1999) 8410–8426.
[23] M. Haruta, N. Yamada, T. Kobayashi, S. Iijima, Journal of Catalysis 115 (1989) 301–309.
[24] M. Haruta, S. Tsubota, T. Kobayashi, H. Kageyama, M.J. Genet, B. Delmon, Journal of Catalysis 144 (1993) 175–192.
[25] A.S.K. Hashmi, G.I. Hutchings, Angewandte Chemie International Edition 45 (2006) 7896–7936.
[26] M. Haruta, Gold Bulletin 37 (2004) 27–36.
[27] M. Haruta, Chemical Record 3 (2003) 75–87.
[28] G.R. Bamwenda, S. Tsubota, T. Nakamura, M. Haruta, Journal of Photochemistry and Photobiology A 89 (1995) 177–189.
[29] H.Y. Lin, Y.S. Chang, International Journal of Hydrogen Energy 35 (2010) 8463–8471.